Perivascular Cells With Pericyte Characteristics Are Involved in ATP- and PGE_2-Induced Relaxation of Porcine Retinal Arterioles In Vitro

Mikkel Wölck Misfeldt, Simon Metz Mariendal Pedersen, and Toke Bek

Department of Ophthalmology, Aarhus University Hospital, Aarhus C, Denmark

Correspondence: Mikkel Wölck Misfeldt, Aarhus University Hospital, Department of Ophthalmology, Norrebrogade 44, 8000 Aarhus C, Denmark; mikkelmisfeldt@gmail.com.

Submitted: January 18, 2013
Accepted: April 5, 2013

Citation: Misfeldt MW, Pedersen SMM, Bek T. Perivascular cells with pericyte characteristics are involved in ATP- and PGE_2-induced relaxation of porcine retinal arterioles in vitro. *Invest Ophthalmol Vis Sci.* 2013;54:3258–3264. DOI:10.1167/iovs.13-11685

Purpose. Relaxation of porcine retinal arterioles in vitro has been shown to be preceded by calcium activity in a population of perivascular cells that cannot be classified as neurons, glial cells, or vascular smooth muscle cells. The purpose of the present investigation was to study calcium activity in these perivascular cells during ATP- and PGE_2-induced vasorelaxation, and to identify pericyte markers and other cellular constituents characterizing these cells.

Methods. Porcine arterioles were loaded with a calcium-sensitive fluorophore and mounted in a myograph. Simultaneous measurements of calcium activity and vascular tone during stimulation with ATP and PGE_2 were performed before and after addition of specific antagonists to these compounds and to nitric oxide. Additionally, immunohistochemistry was performed on whole mounts of porcine retina using antibodies to known markers of vascular pericytes and cellular components of the vascular wall.

Results. Relaxation of retinal arterioles with both ATP and PGE_2 was preceded by a significant increase in the number of perivascular cells displaying calcium activity. The effect of ATP was inhibited by the adenosine receptor antagonist 8-PSPT, whereas the effect of PGE_2 was inhibited by the EP1 receptor antagonist SC19220 and the NO-synthesis inhibitor L-NAME. The perivascular cells had morphological features in common with pericytes and displayed immunoreactivity to the pericyte markers NG2 and CD-13, but not to markers of glial cells, neurons, or vascular smooth muscle cells.

Conclusions. The perivascular cell type located external to the smooth muscle cells in porcine retinal arterioles shows calcium activity during relaxation with ATP and PGE_2 and has morphological properties in common with pericytes. Future studies should focus on the role of this cell type for regulating retinal blood flow and for retinal vascular disease.

Keywords: pericyte, retinal arterioles, calcium, prostaglandin E2, ATP, nitric oxide

Retinal blood flow is regulated by the tone of the vascular smooth muscle cells, but the cellular basis for this regulation is not known in detail. Previous studies have shown that relaxation of retinal arterioles can be induced by ATP and PGE_2 agonistic effects in the perivascular retinal tissue,[1–3] and that PGE_2 may interact with nitric oxide (NO) to facilitate vasorelaxation.[4] Additionally, ATP-induced relaxation has been shown to be preceded by increased calcium activity in a population of perivascular cells (PVCs) that cannot be classified as neurons, glial cells, or smooth muscle cells.[5] However, the interaction between ATP and PGE_2 for activating these perivascular cells is unknown, and it remains to be studied whether these cells have characteristics in common with vascular pericytes.

Therefore, the purpose of the present study was to quantify calcium activity in the unclassified perivascular cell during both ATP- and PGE_2-induced vasorelaxation, and to identify pericyte markers and other morphological characteristics in these cells. Porcine arterioles were loaded with a calcium-sensitive fluorophore and mounted in a myograph. Simultaneous measurements of calcium activity and vascular tone during stimulation with ATP and PGE_2 were performed before and after addition of specific antagonists to these compounds and to NO. Additionally, immunohistochemistry was performed on wholemounts of porcine retina using antibodies to known markers of vascular pericytes and cellular components of the vascular wall.

Materials and Methods

Solutions and Chemicals

Pharmacological Experiments. Solvents: Physiological saline solution (PSS 1.6) containing (in mM): 119 NaCl, 4.7 KCl, 1.17 $MgSO_4 \cdot 7H_2O$, 25 $NaHCO_3$, 1.18 KH_2PO_4, 0.026 EDTA, 1.6 $CaCl_2$, and 5.5 glucose. PSS 0.0 had the same composition as PSS 1.6 except that $CaCl_2$ had been omitted. The solutions were bubbled with a gas mixture composed of 95% atmospheric air and 5% CO_2. The buffer for loading calcium was composed of 7.94 μM Oregon Green bapta 1-AM, 0.33% DMSO (wt/vol), 0.066% cremophor EL (wt/vol), and 0.013% pluronic F-127 (wt/vol).

Chemicals: U46619 (9,11-dideoxy-9α,11α-methanoepoxy prostaglandin $F_{2\alpha}$); prostaglandin E_2 (PGE_2); and 8-chlorodibenz[b,f][1,4]oxazepine-10(11H)-carboxy-(2-acetyl)hydrazide (SC19220) were acquired from AH diagnostics (Aarhus, Den-

mark). 8-(p-Sulfophenyl)theophylline hydrate (8-PSPT); adenosine triphosphate (ATP); L-NG-Nitroarginine methyl ester (L-NAME); dimethyl sulfoxide (DMSO); Cremophor EL; and pluronic F-127 were purchased from Sigma-Aldrich (Brøndby, Denmark). Oregon green bapta 1-AM was obtained from Invitrogen (Nærum, Denmark).

Immunohistochemistry. Solvents: TBS buffer (pH 7.4) containing 50 mM Tris-HCL; 150 mM NaCl; and Coon's buffer (pH 7.4) containing 0.01 M natrium diethylbarbiturate, 0.1 M NaCl, pH 7.4 methanol, BSA, Triton X-100, and saponin were purchased from Sigma-Aldrich. BSA++ was made of a composition of Tris-HCL containing 0.25% BSA, 0.1% Triton X-100, and 0.1% saponin.

Primary antibodies: *Rabbit anti human* Type II transmembrane glycoprotein (CD13); platelet-derived growth factor B (PDGF-B); α-smooth muscle actin, C-kit; desmin; glial fibrillary acidic protein (GFAP); and vimentin. *Mouse anti human* chondroitin sulphate proteoglycan (NG2); myelin basic protein (MBP); α-tubulin; collagen IV; neuron specific enolase (NSE); oligodendrocyte marker O4; synaptophysin; vimentin; and von Willebrand factor (vWF) and antiastrocyte antibody (clone J1-31).

Secondary antibodies: TRITC conjugated *goat anti mouse* IgG F(ab')2; FITC conjugated *goat anti rabbit* IgG F(ab')2 (Invitrogen); and FITC conjugated *donkey anti goat* IgG (Santa Cruz Biotechnology, Inc., Santa Cruz, CA).

Nuclear staining: SYTO 82 (Invitrogen) and 4′,6-diamidino-2-phenylindole (DAPI) were purchased from Sigma-Aldrich.

Tissue

Eyes from domestic Danish pigs were collected at a local slaughterhouse (Danish Crown, Horsens, Denmark) immediately after the animals had been anesthetized with carbon dioxide and killed by exsanguination. The eyes were kept in 4°C PSS 1.6, and postmortem time until the commencement of the pharmacological experiments never exceeded 3 hours. The dissection procedure was carried out in PSS 0.0 as described previously.[6] In short, the eyes were bisected and the vitreous humor was carefully removed. First order arterioles were identified on the basis of the capillary free zone around these vessels. Starting from a location approximately 1 to 2 mm from the optic disk, an arteriolar segment with a length of approximately 2 mm and a zone of perivascular retinal tissue extending approximately 2 mm on each side of the vessel was cut using a self-locking chisel blade handle (VWR International, Herlev, Denmark) equipped with a 30° microblade (BD Beaver; D.J. Instruments, Billerica, MA).

Mounting in Myograph and Confocal Microscope

The arteriolar segment was transferred to a confocal myograph (120 CW, Danish Myo Technology A/S, Aarhus, Denmark) connected to an analog/digital converter for the recording of isometric tone during the experiments as described previously.[7] The mounting procedure was performed in PSS 0.0 using an upright stereo microscope (STEMI 1000; Carl Zeiss Meditec, Jena, Germany); and after mounting, the myograph was placed in a confocal microscope (LSM 5 Pascal; Carl Zeiss Meditec). Each arteriole was normalized using a standard procedure previously described by Hessellund et al.[8] Subsequently, the tissue was loaded with the calcium-sensitive fluorophore Oregon green bapta 1-AM (Invitrogen) for 10 minutes. After loading, the chamber solution was washed three times with PSS 1.6 and the tissue was allowed to equilibrate for 10 minutes before commencing the experiments.

The calcium sensitive fluorophore was excited using an Argon laser at 488 nm and emission was detected at 530 nm.

Pharmacological Experiments

Altogether, 46 arterioles were studied using the following protocol:

1. The adenosine receptor antagonist 8-PSPT (5×10^{-4} M); the prostaglandin E_2 receptor antagonist SC19220 (5×10^{-5} M); the NOS inhibitor L-NAME (10^{-4} M); or none (control) was added to be present throughout the experiment.
2. Contraction was induced by adding 10^{-6} M U46619 to be present throughout the experiment. If the tone failed to increase more than 0.1 N/m, the vessel was considered nonviable and was discarded.
3. Concentration-response experiments were performed with successive addition of PGE_2 in the concentrations (M) 10^{-9}, 10^{-8}, 10^{-7}, 10^{-6} and 10^{-5}, or ATP in the concentrations (M) 10^{-8}, 10^{-7}, 10^{-6}, 10^{-5}, and 10^{-4}.

Data Sampling

Vascular tone was recorded continuously throughout the experiment as described previously.[7] The active tone was defined as the tone increase induced by contraction of the vessel with U46619, and the tone response during the following pharmacological experiments was calculated as the percentage relaxation of the active tone induced by the added agonist. Recording of fluorescence was commenced after each new addition of a compound to the chamber solution, and was performed five times per second for at least 75 seconds, where after the data were stored in a computer for later analysis.

In each preparation, a region of interest (ROI) was selected to include an area of approximately 0.6 mm^2 as previously described[5] and fluorescence inside the perivascular cells in this area was recorded. Each ROI contained on average 34.2 (range: 24–43) perivascular cells ($n = 28$ vessels). The activity of the perivascular cells was calculated as the percentage of cells showing at least 10% increase in the average fluorescence intensity after addition of an agonist, and a number of observations were included that in a post hoc, one-tailed power analysis allowed comparisons between the groups with a statistical power of more than 90%. In 14 cases where the myograph wire and the perivascular cells were in focus out of 31 experiments where relaxation was not antagonized, hyperfluorescence in the perivascular cells was seen to precede vasorelaxation.

Both agonists used in the experiments showed a concentration-dependent decrease in vascular tone accompanied with a simultaneous increase in fluorescence, and in order to study the effects of inhibitors of these responses, the calcium activity and the tone responses at the highest agonist concentration were used for further analysis.

Immunohistochemistry

Tissue. Altogether 74 arterioles with preserved perivascular retinal tissue were studied, of which six arterioles loaded with Oregon green and examined in the confocal myograph were processed further. In these arterioles, calcium loading was combined with nuclear staining using 10^{-6} M SYTO 80 (four arterioles), or fixated in methanol for 10 minutes for subsequent immunohistochemistry (two arterioles).

The remaining 68 arterioles with preserved retinal tissue not initially loaded with Oregon green were dissected from retinal segments with a length of approximately 3 cm containing the primary and secondary arteriole. The arterioles were mounted on glass pipettes and carefully perfused with PSS 1.6 in order to rinse out remaining blood. Subsequently,

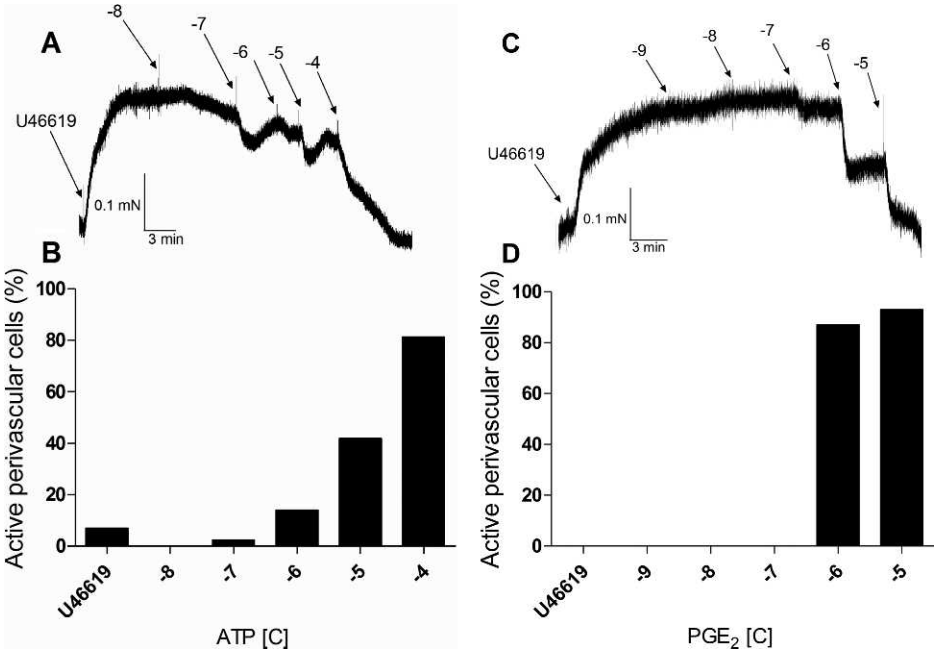

Figure 1. Representative traces of vascular tone (**A**, **C**) and the corresponding percentage of active perivascular cells (**B**, **D**) during addition of ATP and PGE_2.

each segment was divided into four specimens with a length of approximately 5 mm, and transferred to a resin container (Nunc A/S, Roskilde, Denmark), and fixated in methanol for 10 minutes.

Protocol. After fixation, the tissue specimens were washed in PBS (pH 7.4) and endogenous peroxidase activity was blocked by adding BSA++ and 0.1 % H_2O_2 for 1 hour. Hereafter, the specimens were incubated in BSA++ for 72 hours at 4°, each with one of the following primary antibodies (1:100). *Pericyte markers:* Rabbit anti-human type II transmembrane glycoprotein (CD13; $n = 3$); mouse anti-human chondroitin sulphate proteoglycan (NG2; $n = 7$, of which two followed loading with Oregon green); rabbit anti-human PDGF-B ($n = 4$); and rabbit anti-human α-smooth muscle actin ($n = 8$). *Cellular elements:* Mouse anti-human α-tubulin ($n = 6$); mouse anti-human astrocyte marker ($n = 4$); rabbit anti-human C-kit ($n = 2$); mouse anti-human collagen IV ($n = 2$); rabbit anti-human desmin ($n = 8$); rabbit anti-human GFAP ($n = 7$); mouse anti-human neuron specific enolase (NSE; $n = 2$); mouse anti-human oligodendrocyte marker O4 ($n = 2$); mouse anti-MBP ($n = 2$); mouse anti-human synaptophysin ($n = 2$); rabbit anti-human vimentin ($n = 7$); and mouse anti-human von Willebrand factor ($n = 2$).

Subsequently, the segments were washed in Coon's buffer (pH 7.1) and incubated with secondary anti-rabbit FITC or secondary anti-mouse TRITC conjugated antibodies (1:100) in BSA++ for 3 hours at room temperature, followed by repeated washing with Coon's buffer. In 21 arterioles, the first immunohistochemical procedure was repeated using another primary antibody while omitting the blocking of endogenous peroxidase activity with BSA++ and 0.1% H_2O_2. Primary labeling of desmin was combined with labeling of synaptophysin ($n = 2$); GFAP ($n = 3$); the astrocyte marker ($n = 2$), NG2 ($n = 2$); tubulin ($n = 2$); and vimentin ($n = 2$). Primary labeling of α-smooth muscle actin was combined with labeling of NG2 ($n = 2$); α-tubulin ($n = 2$); and vWf ($n = 2$); and primary labeling of NG2 was combined with labeling of CD13 ($n = 2$).

Controls

The specificity of the immunoreactions was controlled by including arterioles where the primary or secondary antibody had been omitted. As positive controls were used: the radial Müller cell processes (GFAP, desmin, and vimentin); vascular endothelial cells (vWF); vascular smooth muscle cells (actin); ganglion cells (NSE and tubulin); basement membrane (collagen IV); mesenteric nerves (S-100 protein, MBP); cerebral oligodendrocytes (oligodendrocyte marker O4) and astrocytes (anti astrocyte antibody).

The arterioles were placed on a tissue slide in 6 × 6 mm in wells formed by a quick-hardening mounting medium (Eukitt; VWR International), were fixated with tissue mounting medium (DAKO, Glostrup, Denmark), and were sealed with a coverslip. The FITC conjugated secondary antibodies were excited similarly to the excitation of Oregon green Bapta 1-AM, whereas the TRITC conjugated secondary antibodies and the nuclear stain SYTO 82 were excited using a He/Ne laser in the confocal microscope at 543-nm line and a long pass filter with a cutoff limit at 560 nm.

The 12-bit monochromatic images of the immunohistochemical reactions were superimposed in respectively the green (FITC and Oregon green) and the red (TRITC) layers of a RBG color image using a Java-based software program (ImageJ; National Institutes of Health [NIH], Bethesda, MD).

Statistical Methods. For each intervention, Student's paired *t*-test was used to test whether ATP and PGE at the highest concentration induced significant relaxation and change in the percentage of active cells compared with the response induced by U46619. Subsequently, one-way ANOVA was used to compare relaxation and change in percentage of active cells between the different interventions, followed by Dunnett's multiple comparison test to identify which intervention(s) induced a response that deviated significantly from the others.

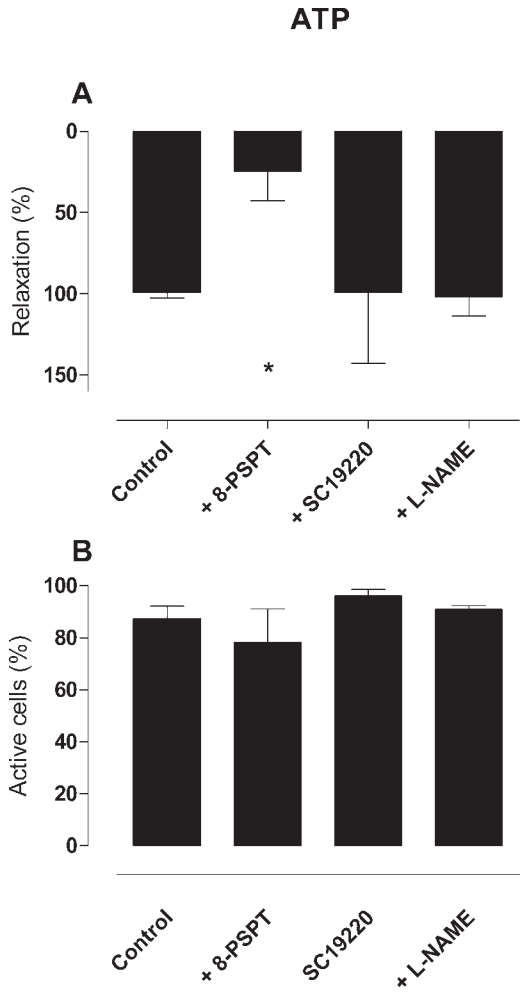

FIGURE 2. (**A**) The change in vascular tone after addition of the highest ATP concentration alone ($n = 10$), or in the presence of 8-PSPT ($n = 6$); SC19220 ($n = 4$); or L-NAME ($n = 4$). (**B**) The corresponding percentage of active perivascular cells. Column heights and *error bars* indicate mean ± SEM. *Asterisk* indicates column that deviates significantly from the others.

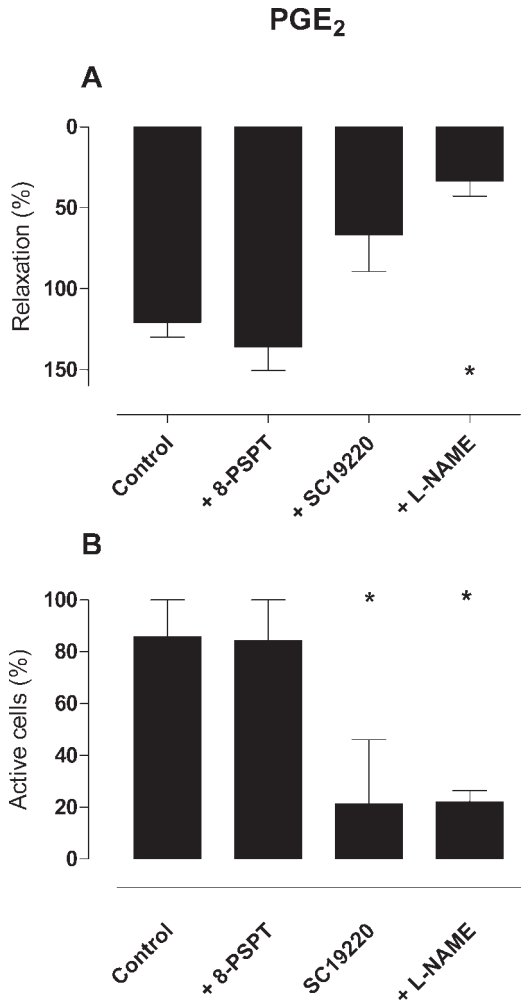

FIGURE 3. (**A**) The change in vascular tone after addition of the highest PGE_2 concentration alone ($n = 6$), or in the presence of 8-PSPT ($n = 5$); SC19220 ($n = 6$); or L-NAME ($n = 5$). (**B**) The corresponding percentage of active perivascular cells. Column heights and *error bars* indicate mean ± SEM. *Asterisks* indicate column(s) that deviate significantly from the others.

RESULTS

Figure 1 shows representative traces of changes in vascular tone and the corresponding percentage of active perivascular cells during concentration-response experiments with the used agonists. It appears that PGE_2 induced full relaxation within a narrower concentration range than ATP.

Figure 2 shows the relaxation of the arterioles and the percentage of active perivascular cells after addition of the highest concentration of ATP. Figure 2A shows that ATP induced a significant relaxation of the retinal arterioles alone (control) and in the presence of the EP1 receptor antagonist SC19220 and the NOS inhibitor L-NAME ($P < 0.01$, for all comparisons), but not in the presence of the adenosine receptor antagonist 8-PSPT ($P = 0.15$). One-way ANOVA showed a significant difference between the groups ($P < 0.01$), which was due to the significantly reduced relaxation after addition of 8-PSPT. Figure 2B shows that ATP significantly increased the number of active perivascular cells ($P < 0.01$), but there was no significant difference in the response between the groups.

Figure 3 shows the relaxation of the arteriole and the percentage of active perivascular cells after addition of the highest concentration of PGE_2. Figure 3A shows that PGE_2 induced a significant relaxation of retinal arterioles alone (control), in the presence of the adenosine receptor antagonist 8-PSPT ($P < 0.01$ for both comparisons), and in the presence of the NO synthesis inhibitor L-NAME ($P = 0.02$), but not in the presence of the EP1 receptor antagonist SC19220 ($P = 0.054$). One-way ANOVA showed a significant difference between the groups ($P < 0.01$), which was due to a significantly reduced relaxation after addition of the NO-synthesis inhibitor L-NAME. Figure 3B shows that PGE_2 significantly increased the percentage of perivascular cells when added alone (control) and in the presence of 8-PSPT ($P < 0.01$ for both comparisons), but not after the addition of SC19220 ($P = 0.065$) or L-NAME ($P = 0.053$) (Supplementary Movie S1). One-way ANOVA shoved a significant difference between the change in activity among the four groups ($P < 0.01$), which was due to a significantly lower response after addition of SC19220 and L-NAME than in the other two groups.

Figure 4 shows the labeling of perivascular cells and adjoining structures: cells loading Oregon green (Fig. 4A); the same slide with cells displaying immunoreactivity to the pericyte marker NG2 (red, Fig. 4B); and superimposition of the two images showing that the labels for calcium activity and

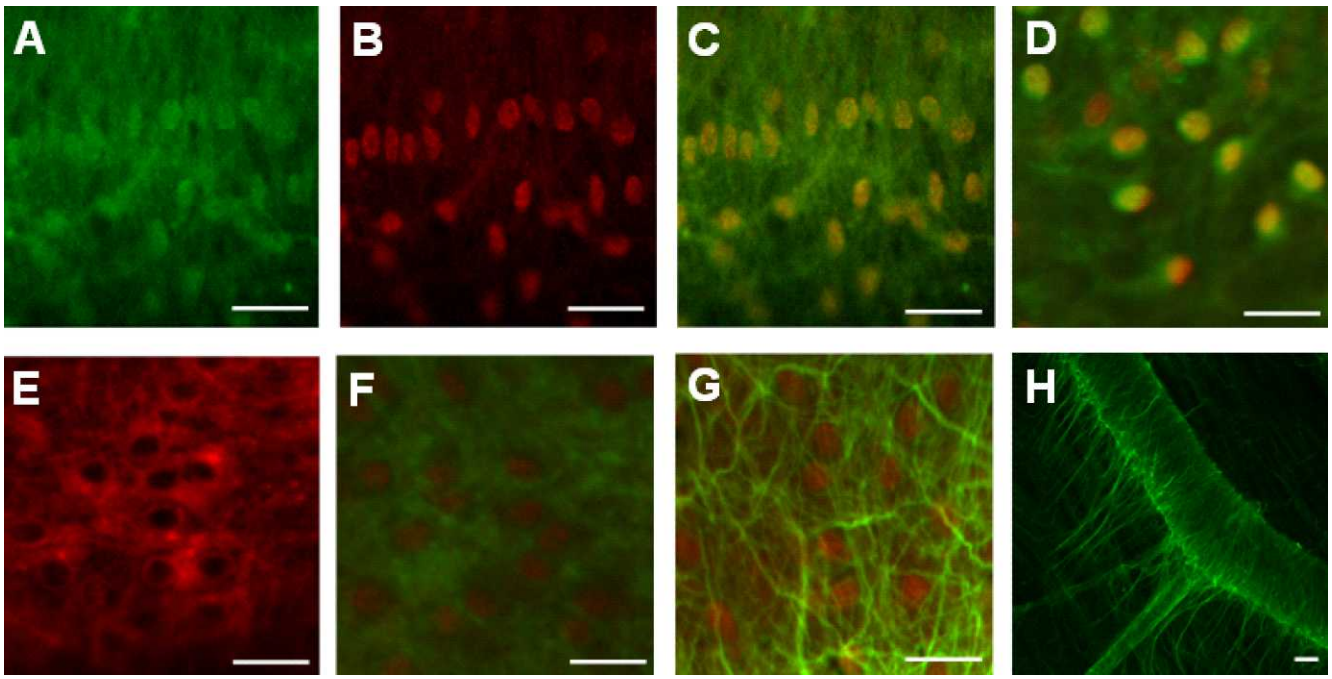

FIGURE 4. Morphological characterization of the perivascular cells. *Scale bars* represent 20 μM. (**A**) The perivascular cells loaded with Oregon green (*green*). (**B**) Immunoreactivity to the pericyte marker NG2 (*red*). (**C**) Superimposition of (**A**) and (**B**) to result in a yellowing of the perivascular cells. (**D**) The labeling with Oregon green also coincided with nucleus staining using SYTO 82 (*yellow*), but the two stainings were separated by procedures that distorted the tissue and an accurate superimposition could not be achieved. (**E**) Circular structures displayed immunoreactivity to tubulin (*red*). (**F**) These circular structures also displayed immunoreactivity to CD-13 (*green*) and encircled the NG2-positive structures (*red*). (**G**) The NG2 immunoreacting structures (*red*) were bounded by processes displaying immunoreactivity to the microfilament desmin (*green*). (**H**) The desmin-positive filaments extended into the perivascular retinal tissue beyond the level of penetration of the used antibodies and calcium markers.

pericytes marked the same structures (yellow, Fig. 4C). The labeling with Oregon green also coincided with the nucleus stainings SYTO 82 (yellow, Fig. 4D) and DAPI (not shown). The layer of perivascular cells contained circular structures displaying immunoreactivity to the cytoskeleton marker tubulin (green, Fig. 4E). This circular zone also showed immunoreactivity to the pericyte marker CD-13 (green) that encircled the NG2 positive structures (red, Fig. 4F). The NG2 immunoreacting structures were bounded by processes displaying immunoreactivity to the microfilament desmin (Fig. 4G). This microfilament extended into the perivascular retinal tissue beyond the level of penetration of the antibodies and calcium markers (Fig. 4H). The perivascular cell structures showed no immunoreactivity to any of the other antibodies used.

DISCUSSION

The present study has shown that a population of PVCs in porcine retinal arterioles display increased intracellular calcium activity during vasorelaxation induced by ATP and PGE_2, and that this cell type has structural characteristics in common with vascular pericytes.

The study confirms previous findings that ATP-induced relaxation of porcine retinal arterioles with preserved perivascular tissue is accompanied by increased calcium activity in the PVC, that relaxation but not calcium activity is inhibited by blocking ATP degradation,[5] and that the relaxing effect of ATP can be blocked by the adenosine receptor antagonist 8-PSPT.[2] Other studies have shown that the relaxing effect of adenosine and ATP on retinal arterioles depends on K_{ATP} channels,[9,10] that are also involved in relaxation induced by lactate and hypoxia.[9–11] Additionally, the present finding that the adenosine antagonist 8-PSPT had no effect on calcium activity in the PVC is in accordance with evidence that the relaxing effect of adenosine is independent of the perivascular tissue and is exerted directly on the vascular smooth muscle cells.[2] Conversely, after blocking of the EP1 receptor with the specific antagonist SC19220 and of NO synthesis using L-NAME, PGE_2 neither had an effect on vascular tone nor on calcium activity in the PVC. This is consistent with a study where SC19220 was found to inhibit ATP-induced relaxation at low but not high ATP concentrations.[1] The lack of blocking of ATP-induced relaxation at high concentrations in the presence of SC19220 and L-NAME may be due to the fact that the effects of these antagonists are in the retinal tissue external to the PVC and the vascular smooth muscle cells, but does not rule out an indirect effect on the vascular wall. Therefore, the findings do not point to the origin of the involved NO. This is supported by the finding that PGE_2-induced relaxation of porcine retinal arterioles and the increased calcium activity in the PVC were both inhibited by SC19220 and L-NAME, although the antagonistic effect of SC19220 was a right shift of the concentrations-response curve so that PGE_2-induced vasorelaxation was antagonized significantly at intermediate but incompletely at high concentrations as shown previously.[1] Assuming that the relaxing effects of ATP and PGE_2 involve separate pathways, the activation of the PVC might represent a more generalized mechanism for mediating relaxation of retinal arterioles. It might therefore be interesting to study whether stimulation of the PVC by different agonists might reveal different response characteristics in the PVC, such as differences in intracellular calcium recruitment.[5,12] The

Investigative Ophthalmology & Visual Science

complexity of the regulation of retinal vascular tone is underlined by the finding that purines can increase intracellular Ca^{2+} in retinal pericytes and induce constriction of retinal microvessels mediated by both P2X and P2Y receptors.[13,14] Other studies have shown that pericytes may be involved in both contraction and dilatation of retinal capillaries,[4,15,16] and that the diameter of retinal capillaries is regulated by mechanisms that involve both purines, prostaglandins, and NO.[15,17–20] However, it is unknown whether these findings on the capillary network can be extrapolated to the larger retinal arterioles known to have distinctly different response properties to vasoactive compounds than their smaller counterparts.[21]

The immunohistochemical experiments indicate that the PVC structure displaying calcium activity to ATP and PGE_2 that precedes relaxation represents the nucleus of a cell with a shallow rim of cytoplasm and is connected to processes extending into the retina. The increased intracellular calcium activity during stimulation with ATP and PGE_2 resembled the response observed by others in glial cells,[18,19,22–24] but the immunoreactions were consistent with previous observations that the PVC is not a glial cell type.[5] Recently, the synantocyte/NG2-glia has been described as a special cell type displaying immunoreactivity to NG2, PDGF-αR, and oligodendrocyte epitopes[25–27] and having an irregular shape with fine dendritic processes located around the nerve fibers. This description does not fit in with the observed perivascular cell because of its lack of immunoreactivity to the specific oligodendrocyte marker (O4) and to the myelin basic protein,[24,28] and because its round structure with morphological characteristics is more in common with pericytes.[29] Generally, pericytes are identified by the presence of immunoreactivity to a subset of one or more pericyte markers depending on the tissue and species involved.[29–31] The present observation of immunoreactivity to NG2 and CD13 antigen in the perivascular cells might therefore be an example of such a tissue-specific subset of markers. Pericytes are typically observed on capillary vessels in a pattern resembling "bumps on a log,"[32] with a primary role of regulating the capillary diameter. Therefore, it might be hypothesized that the perivascular cells characterized in the present study could be pericytes modified to regulate the tone of larger retinal arterioles. This might explain why these cells are lacking some of the normal characteristics of capillary pericytes such as actin, which is superfluous in larger arterioles with an abundance of vascular smooth muscle cells specialized to contract the vessel.

One of the hypotheses for the development of diabetic retinopathy is that the diabetic metabolic dysregulation leads to loss of retinal capillary pericytes with consequent occlusion of the capillaries to result in retinal ischemia.[33–39] It is possible that similar changes can occur in the larger retinal vessels, where dysfunction of the PVC may contribute to the dilatation of retinal arterioles and the consequent retinal hyperperfusion observed clinically in patients with diabetic retinopathy.[40,41] Therefore, future studies should investigate the distribution of PVC in retinal arterioles from animal models of diabetic retinopathy and in postmortem tissue from patients with diabetic retinopathy.

In conclusion, the findings of the present study have shown that the perivascular cell type located in a vimentin-positive layer external to the smooth muscle cells and internal to glial cells in retinal arterioles shows calcium activity during relaxation with ATP and PGE_2 and has morphological and immunohistochemical properties in common with pericytes. Future studies should focus on the role of this cell type in retinal vascular physiology by elucidating how different vasoactive compounds interact on the cell to change vascular tone, how calcium is recruited in this cell, and how the cell is connected to the perivascular retina. Additionally, studies should aim at elucidating the role of the PVC for vascular pathophysiology, notably diabetic retinopathy where changes in retinal flow regulation are involved in the disease pathogenesis.

Acknowledgments

Supported by the VELUX Foundation, the Danish Medical Research Council, Boehm's Foundation, and Jochum and Marie Jensen's Foundation.

Disclosure: **M.W. Misfeldt**, None; **S.M.M. Pedersen**, None; **T. Bek**, None

References

1. Holmgaard K, Bek T. ATP-induced relaxation of porcine retinal arterioles in vitro depends on prostaglandin E synthesized in the perivascular retinal tissue. *Invest Ophthalmol Vis Sci*. 2010;51:5168–5175.
2. Holmgaard K, Aalkjaer C, Lambert JD, Bek T. ATP-induced relaxation of porcine retinal arterioles depends on the perivascular retinal tissue and acts via an adenosine receptor. *Curr Eye Res*. 2007;32:353–359.
3. Holmgaard K, Aalkjaer C, Lambert JD, Hessellund A, Bek T. The relaxing effect of perivascular tissue on porcine retinal arterioles in vitro is mimicked by N-methyl-D-aspartate and is blocked by prostaglandin synthesis inhibition. *Acta Ophthalmol*. 2008;86:26–33.
4. Gordon GR, Howarth C, MacVicar BA. Bidirectional control of arteriole diameter by astrocytes. *Exp Physiol*. 2011;96:393–399.
5. Misfeldt MW, Aalkjaer C, Simonsen U, Bek T. Novel cellular bouton structure activated by ATP in the vascular wall of porcine retinal arterioles. *Invest Ophthalmol Vis Sci*. 2010;51:6681–6687.
6. Jeppesen P, Aalkjaer C, Bek T. Bradykinin relaxation in small porcine retinal arterioles. *Invest Ophthalmol Vis Sci*. 2002;43:1891–1896.
7. Misfeldt MW, Aalkjaer C, Simonsen U, Bek T. Voltage-gated calcium channels are involved in the regulation of calcium oscillations in vascular smooth muscle cells from isolated porcine retinal arterioles. *Exp Eye Res*. 2010;91:69–75.
8. Hessellund A, Jeppesen P, Aalkjaer C, Bek T. Characterization of vasomotion in porcine retinal arterioles. *Acta Ophthalmol Scand*. 2003;81:278–282.
9. Jeppesen P, Aalkjaer C, Bek T. Adenosine relaxation in small retinal arterioles requires functional Na-K pumps and K(ATP) channels. *Curr Eye Res*. 2002;25:23–28.
10. Nakaizumi A, Puro DG. Vulnerability of the retinal microvasculature to hypoxia: role of polyamine-regulated K(ATP) channels. *Invest Ophthalmol Vis Sci*. 2011;52:9345–9352.
11. Hein TW, Xu W, Kuo L. Dilation of retinal arterioles in response to lactate: role of nitric oxide, guanylyl cyclase, and ATP-sensitive potassium channels. *Invest Ophthalmol Vis Sci*. 2006;47:693–699.
12. Bek T, Holmgaard K. GABA-induced relaxation of porcine retinal arterioles in vitro depends on inhibition from the perivascular retina and is mediated by GABAC receptors. *Invest Ophthalmol Vis Sci*. 2012;53:3309–3315.
13. Kawamura H, Sugiyama T, Wu DM, et al. ATP: a vasoactive signal in the pericyte-containing microvasculature of the rat retina. *J Physiol*. 2003;551:787–799.
14. Peppiatt CM, Howarth C, Mobbs P, Attwell D. Bidirectional control of CNS capillary diameter by pericytes. *Nature*. 2006;443:700–704.

15. Hamilton NB, Attwell D, Hall CN. Pericyte-mediated regulation of capillary diameter: a component of neurovascular coupling in health and disease. *Front Neuroenergetics*. 2010;2:5.
16. Gordon GR, Mulligan SJ, MacVicar BA. Astrocyte control of the cerebrovasculature. *Glia*. 2007;55:1214–1221.
17. Zonta M, Angulo MC, Gobbo S, et al. Neuron-to-astrocyte signaling is central to the dynamic control of brain microcirculation. *Nat Neurosci*. 2003;6:43–50.
18. Metea MR, Newman EA. Glial cells dilate and constrict blood vessels: a mechanism of neurovascular coupling. *J Neurosci*. 2006;26:2862–2870.
19. Metea MR, Newman EA. Calcium signaling in specialized glial cells. *Glia*. 2006;54:650–655.
20. Filosa JA, Bonev AD, Nelson MT. Calcium dynamics in cortical astrocytes and arterioles during neurovascular coupling. *Circ Res*. 2004;95:e73–e81.
21. Yamanishi S, Katsumura K, Kobayashi T, Puro DG. Extracellular lactate as a dynamic vasoactive signal in the rat retinal microvasculature. *Am J Physiol Heart Circ Physiol*. 2006;290:H925–H934.
22. Butt AM. ATP: a ubiquitous gliotransmitter integrating neuron-glial networks. *Semin Cell Dev Biol*. 2011;22:205–213.
23. Hamilton N, Vayro S, Kirchhoff F, et al. Mechanisms of ATP- and glutamate-mediated calcium signaling in white matter astrocytes. *Glia*. 2008;56:734–749.
24. Hamilton N, Vayro S, Wigley R, Butt AM. Axons and astrocytes release ATP and glutamate to evoke calcium signals in NG2-glia. *Glia*. 2010;58:66–79.
25. Berry M, Hubbard P, Butt AM. Cytology and lineage of NG2-positive glia. *J Neurocytol*. 2002;31:457–467.
26. Butt AM, Hamilton N, Hubbard P, Pugh M, Ibrahim M. Synantocytes: the fifth element. *J Anat*. 2005;207:695–706.
27. Butt AM, Kiff J, Hubbard P, Berry M. Synantocytes: new functions for novel NG2 expressing glia. *J Neurocytol*. 2002;31:551–565.
28. Baumann N, Pham-Dinh D. Biology of oligodendrocyte and myelin in the mammalian central nervous system. *Physiol Rev*. 2001;81:871–927.
29. Dore-Duffy P. Pericytes: pluripotent cells of the blood brain barrier. *Curr Pharm Des*. 2008;14:1581–1593.
30. Balabanov R, Dore-Duffy P. Role of the CNS microvascular pericyte in the blood-brain barrier. *J Neurosci Res*. 1998;53:637–644.
31. Shepro D, Morel NM. Pericyte physiology. *FASEB J*. 1993;7:1031–1038.
32. Yemisci M, Gursoy-Ozdemir Y, Vural A, Can A, Topalkara K, Dalkara T. Pericyte contraction induced by oxidative-nitrative stress impairs capillary reflow despite successful opening of an occluded cerebral artery. *Nat Med*. 2009;15:1031–1037.
33. Bek T. Immunohistochemical characterization of retinal glial cell changes in areas of vascular occlusion secondary to diabetic retinopathy. *Acta Ophthalmol Scand*. 1997;75:388–392.
34. Bek T. Glial cell involvement in vascular occlusion of diabetic retinopathy. *Acta Ophthalmol Scand*. 1997;75:239–243.
35. Kringelholt S, Simonsen U, Bek T. Dual effect of prostaglandins on isolated intraocular porcine ciliary arteries [published online ahead of print August 3, 2012]. *Acta Ophthalmol*. doi:10.1111/j.1755-3768.2012.02479.x.
36. Chibber R, Molinatti PA, Rosatto N, Lambourne B, Kohner EM. Toxic action of advanced glycation end products on cultured retinal capillary pericytes and endothelial cells: relevance to diabetic retinopathy. *Diabetologia*. 1997;40:156–164.
37. Puro DG. Physiology and pathobiology of the pericyte-containing retinal microvasculature: new developments. *Microcirculation*. 2007;14:1–10.
38. Bek T. Transretinal histopathological changes in capillary-free areas of diabetic retinopathy. *Acta Ophthalmol (Copenh)*. 1994;72:409–415.
39. Addison DJ, Garner A, Ashton N. Degeneration of intramural pericytes in diabetic retinopathy. *Br Med J*. 1970;1:264–266.
40. Bek T, Jeppesen P, Kanters JK. Spontaneous high frequency diameter oscillations of larger retinal arterioles are reduced in type 2 diabetes mellitus. *Invest Ophthalmol Vis Sci*. 2013;54:636–640.
41. Kristinsson JK, Gottfredsdottir MS, Stefansson E. Retinal vessel dilatation and elongation precedes diabetic macular oedema. *Br J Ophthalmol*. 1997;81:274–278.

Investigative Ophthalmology & Visual Science